ISSN 1573-160X, *PHYSICAL OCEANOGRAPHY*, Vol. 32, Iss. 3, pp. 372-391 (2025)

published in *Morskoy Gidrofizicheskiy Zhurnal*, 2025, Vol. 41, Iss. 3, pp. 358–377

Original article

Model of the Lagrangian Particle Transport in a Quasi-Two-Phase Ocean – Ice Medium in a Parallel Ocean Dynamics Model

S. V. Semin [1, 2, ✉], L. Yu. Kalnitskii [1], K. V. Ushakov [1], R. A. Ibrayev [3, 1]

[1] *Shirshov Institute of Oceanology, Russian Academy of Sciences, Moscow, Russian Federation*
[2] *Nuclear Safety Institute, Russian Academy of Sciences, Moscow, Russian Federation*
[3] *Marchuk Institute of Numerical Mathematics, Russian Academy of Sciences, Moscow, Russian Federation*
✉ *svsemin@unistemlab.com*

Abstract
Purpose. The purpose of the study is to develop the model of impurity transport in the ocean – sea ice system based on the Lagrangian approach.
Methods and Results. The Lagrangian transport of particles is considered in the approximation of a quasi-two-phase ocean – ice medium (particles are subject to the ice formation and melting processes, but actually remain in the ocean model). For the first time, the Lagrangian model over an arbitrary computational grid taking into account the quadratic correction of turbulent diffusion is described in detail. A synchronous model for the Lagrangian transport and the ocean – sea ice model (INMIO – CICE5.1) is constructed. The test calculations of particle transport in the field of a static vortex in the Cartesian and spherical coordinate systems demonstrate the correctness of the presented method. The results of the experiment on particle cloud transport in the Laptev Sea have shown both the fundamental possibilities of using the approach to solve applied problems and a good scalability of the model's parallel implementation for a large (up to 10^6) number of particles.
Conclusions. The model developed on the basis of the Eulerian and Lagrangian approaches, makes it possible to solve comprehensively the problems related to water circulation and spread of impurities of various types (radioactive and stable isotopes, soluble and insoluble elements of anthropogenic and natural origin, etc.) and, consequently, to assess their impact on the environment.

Keywords: computer modeling, Lagrangian transport, ocean dynamics model, ocean – ice model, two-phase medium, turbulent mixing, parallel calculations

Acknowledgments: The work was conducted at the Nuclear Safety Institute, RAS, with financial support from the Russian Science Foundation (grant No. 20-19-00615, sections 2-5), and at the Shirshov Institute of Oceanology, RAS, under state assignment theme FMWE-2024-0017 (section 1). Computational resources were provided by the Interdepartmental Supercomputer Center, RAS.

For citation: Semin, S.V., Kalnitskii, L.Yu., Ushakov, K.V. and Ibrayev, R.A., 2025. Model of the Lagrangian Particle Transport in a Quasi-Two-Phase Ocean – Ice Medium in a Parallel Ocean Dynamics Model. *Physical Oceanography*, 32(3), pp. 372-391.

Introduction

Two traditional approaches are conventionally used when solving hydrodynamic problems: the Eulerian approach and the Lagrangian approach. These methods are generally effective for different classes of problems and have a wide range of applications. They can also complement each other to provide a more

complete picture of processes occurring in the fluid. The Eulerian approach is mainly used when constructing most modern ocean circulation models and when describing the general dynamics of a continuous medium. By contrast, the Lagrangian approach involves tracking the trajectory of an infinitesimal fluid particle in the presence of specified forces. This makes it possible to evaluate the details of individual currents or specific structures (for example, surface and underwater currents, oceanic vortices) during the evolution of the internal state of the continuous medium. It also enables the evaluation of specific features of currents or particular structures (such as surface and subsurface currents, oceanic vortices, etc.) during the evolution of the continuum medium's internal state. At the same time, various properties can be assigned to the particles, including characteristic of local biogenic and anthropogenic processes and real or hypothetical sources of pollution, including radioactive ones. This allows the dynamics of impurity propagation in a given current to be reconstructed. Since ocean dynamics modeling often considers water in two states (liquid and solid), the dynamic properties of which are fundamentally different, studying particle transport within both thermodynamic phases is of particular scientific interest. To the best of our knowledge, there are currently no publicly available models that consider such processes [1].

Combining Eulerian and Lagrangian approaches provides comprehensive solutions to problems involving water circulation and the dispersion of various types of impurities (radioactive and stable isotopes, soluble and insoluble elements of anthropogenic and natural origin). Consequently, it is possible to assess their environmental impact. This tool is particularly relevant due to the development of the Northern Sea Route [1] and the Arctic region [2] as a whole in terms of logistical and military-political potential. Floating nuclear power plants are already being actively utilized during the development of resources in the Arctic Ocean (AO). Due to various risk factors, a detailed study of their environmental impact is necessary [2]. Particular attention should be given to potential emergency situations involving the release of radioactive isotopes into the AO waters. Research is required to assess the long-term consequences of such an event [3]. A tool based on a coupled Lagrangian-Eulerian ocean model would be optimally suited to solving these problems. In this context, developing such a tool using domestic software platforms is particularly relevant [3].

When developing coupled Lagrangian-Eulerian models, particles are typically treated as passive tracers that do not affect the properties of the carrying flow. In such configurations, the Eulerian model is primary in the sense that the accuracy and reliability of the calculated velocity field determine the predictability of particle transport. The Eulerian ocean dynamics model involves the numerical solution of

[1] Government of the Russian Federation, 2019. [*Northern Sea Route Infrastructure Development Plan until 2035 (Order No. 3120-r of December 21, 2019). Collected Legislation of the Russian Federation*]. No. 52 (Part V), Article 8053 (in Russian).

[2] Government of the Russian Federation, 2021. [*Socio-Economic Development of the Arctic Zone of the Russian Federation. Resolution of the Government of the Russian Federation No. 484, 30 March. Collected Legislation of the Russian Federation*]. No. 14, Article 2411 (in Russian).

[3] Government of the Russian Federation, 2023. [*Concept of Technological Development until 2030. Order of the Government of the Russian Federation No. 1315-r, 20 May, Moscow*] (in Russian).

the full set of fluid dynamics equations for a specified body of water with a defined spatial resolution, as well as the parameterization of internal and boundary processes. Coupling this approach with ice and/or atmospheric models demonstrates its high effectiveness in forecasting regional and global climate dynamics [4–10]. Combining such models with Lagrangian transport modeling is the most appropriate approach, as evidenced by the numerous existing implementations reviewed in [1].

There are two subclasses of numerical models that support Lagrangian particle transport: autonomous and synchronous. In the former, the Eulerian and Lagrangian models run independently of each other (usually sequentially). The velocity field obtained from the first model is then used in the second model. Examples of the first subclass include TRACMASS [11], Ariane [12], CMS [13], and the SibCIOM-based Lagrangian model [14]. In the second subclass, the modeling of fluid dynamics and particles is carried out synchronously. The complete set of current data for the entire computational domain is used in the Lagrangian model at each time step, providing the maximum possible temporal resolution. Examples of implementations can be found in the MRI.COM [4], NEMO [5], HYCOM [15], ROMS [16], and MITgcm [17] models.

Compared to synchronous models, autonomous models have several disadvantages. Specifically, three-dimensional velocity fields are always time-averaged (and sometimes spatially averaged), which reduces the accuracy with which dynamic processes can be described [1]. Storing current data in four-dimensional arrays requires substantial disk space. This limits the ability to study temporally extended and spatially detailed processes. Secondly, reading data from external storage is a relatively slow process that significantly impacts post-processing performance and the computational efficiency of the autonomous model. While synchronous models offer many advantages, they also have certain drawbacks, including placing an additional load on high-performance computing system resources and making implementation somewhat more complex.

The aim of this work is to develop and implement a Lagrangian transport model within the INMIO ocean dynamics model [18], which forms part of the integrated ocean – ice – atmosphere – land modeling system [5, 6, 9, 19]. The Lagrangian particle transport model must have the following features: synchronous execution with the ocean dynamics model, incorporation of two-phase transport capability for ocean – ice system simulations, enabling of particle injection at specified coordinates and times, support for particle classification into groups based on individual properties (including lifetime duration, buoyancy characteristics, and bottom adhesion conditions), a total number of particles of up to 10^6.

[4] Sakamoto, K., Nakano, H., Urakawa, S., Toyoda, T., Kawakami, Y., Tsujino, H. and Yamanaka, G., 2023. *Reference Manual for the Meteorological Research Institute Community Ocean Model Version 5 (MRI.COMv5)*. MRI, 334 p. (Technical Reports of the Meteorological Research Institute; No. 87).

[5] Madec, G. and the NEMO Team, 2016. *NEMO Ocean Engine: Technical Report*. 300 p. (Note du Pôle de Modélisation de l'Institut Pierre-Simon Laplace; No. 27). https://doi.org/10.5281/ZENODO.3248739

Data and methods

Coupled ocean – ice model. The implementation of a synchronous Lagrangian transport model depends directly on the 'parent' Eulerian model and its specific architecture. This study focuses on developing a particle transport model for a two-phase medium, representing aspects that are particularly important from the standpoint of the Lagrangian model for implementing both components in the ocean – ice modeling system.

The basic ocean model of the joint modeling complex is represented by the INMIO numerical model of ocean dynamics [18]. This model belongs to the 3D PEM (3-Dimensional Primitive Equation Models) class. It is based on the classical system of Reynolds equations under the Boussinesq, hydrostatic and incompressible fluid approximations. The free boundary of the atmosphere – ocean interface is described by a nonlinear kinematic condition that explicitly describes the flows of water, heat, salt and momentum. At rigid boundaries, the free-slip condition and zero heat and salinity flow are specified.

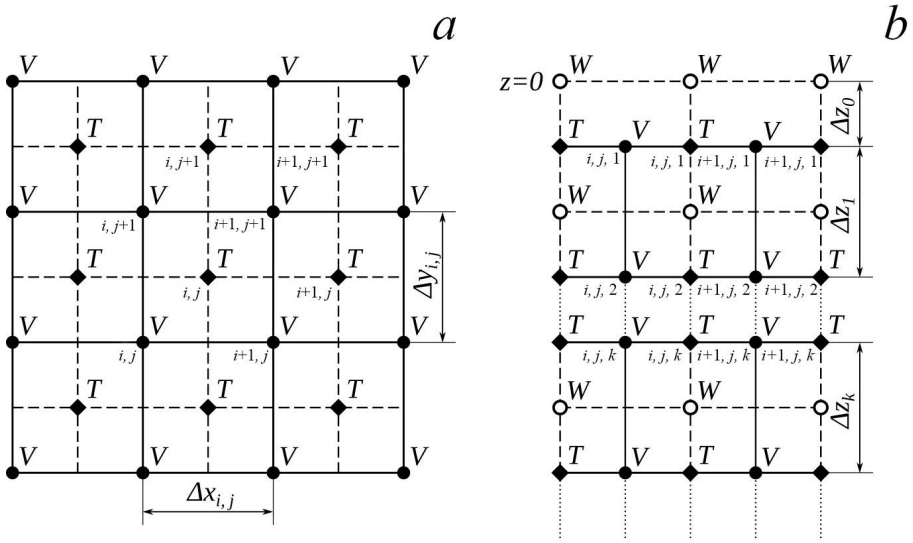

F i g. 1. Calculation grid in the INMIO model: scheme of the arrangement of grid nodes in the horizontal (*a*) and vertical (*b*) planes

The original differential equations are approximated using the finite volume method on a *B*-type horizontal grid (Fig. 1), which uses *z*-coordinates in the vertical dimension and an arbitrary orthogonal coordinate system in the horizontal plane. Currently, Cartesian, spherical and tripolar coordinate systems are supported. The numerical model is optimized for parallel execution on high-performance computing systems via two-dimensional domain decomposition.

The coupled ocean – ice model incorporates sea ice dynamics via the CICE5.1 model [6]. It characterizes the state of ice and snow using a distribution function

[6] Hunke, E.C. and Lipscomb, W.H., 2013. *CICE: The Los Alamos Sea Ice Model Documentation and Software User's Manual Version 5.1. LA-CC-06-012*. Los Alamos National Laboratory, 115 p.

$g(t, x, h)$ that depends on time, geographical coordinates and ice thickness. The primary prognostic variables include ice concentration, averaged thickness values, the internal energy of ice and snow, ice salinity, temperature, and the ice velocity vector. The original thermodynamic and ice transport equations are approximated using the finite difference method on a *B*-type grid in Cartesian, polar or tripolar coordinate systems at the ocean surface.

The coupled ocean – ice modeling system has been implemented using the compact computational platform CMF3.0 [5]. In addition to centralized and parallel input/output operations, CMF3.0 integrates multiple models into a unified geophysical modeling system by reinterpolating the components participating in modeling onto different grids.

Based on the abovementioned information, more detailed requirements for implementing the Lagrangian model can be formulated. The implementation must support centralized input/output with specified discretization through CMF3.0 procedures. As the formulation of the ocean – ice system does not include the transport of particles into the atmosphere, it is sufficient to implement support for Lagrangian transport in the ocean model, ensuring the reinterpolation of the velocity field and the ice formation/melting potential from the ice model using the compact computational platform's method. Finally, as the INMIO model is defined in an arbitrary orthogonal coordinate system, the Lagrangian model must support particle transport in any coordinate system.

Taking these requirements into account, the procedure for calculating the trajectories of Lagrangian particles in the ocean model can be represented as two fundamental operations: the interpolation of the discrete velocity field to an arbitrary coordinate point (particle coordinates) within a specific coordinate system; and the integration of the equation describing the motion of the particles in the given current field.

The model of Lagrangian particle transport. As mentioned in the introduction, from a practical standpoint, it is interesting to track not only the movement of water, but also that of dissolved trace elements in the ocean, such as radionuclides, nutrients, plankton and minerals. However, it is insufficient to simply compute the displacement of fluid particles under the influence of a given velocity field, since the mass of dissolved material in a given volume is generally not constant due to turbulent mixing. As small-scale processes are difficult to describe within the framework of a general ocean circulation model, the mixing effect must be represented directly in the Lagrangian model as particle transport under the influence of diffusion [1]. Thus, the Lagrangian model accounts for the transport of a fluid particle with fixed physical properties within a given velocity field, taking into account the effects of turbulent mixing. The concentration of dissolved material can then be determined by counting the number of particles in a given volume. This approach was first introduced in [20] and has since become standard practice for modeling dissolved substance transport [1].

Since turbulent mixing processes are random by nature and liquid particle transport and diffusion are assumed to be linearly independent processes, stochastic differential equations can be used to model Lagrangian transport. In general, this equation is represented by formula (1). This is a stochastic differential equation,

which is a special case of the Langevin equation. The additional term in this equation describes the random fluctuations of a particle caused by turbulent processes [21]:

$$\frac{d\vec{x}(t)}{dt} = \vec{A}(\vec{x}, t) + B(\vec{x}, t)\vec{L}(t), \quad (1)$$

where $\vec{x}(t) = \left(x^l(t), y^l(t), z^l(t)\right)$ are the coordinates of a particle in a given space; $\vec{A}(\vec{x}, t)$ is a vector representing a deterministic force field that governs the evolution of $\vec{x}(t)$; $B(\vec{x}, t)$ is a predefined tensor that characterizes the stochastic influence on the particle (in this case, turbulence); $\vec{L}(t)$ is a random vector representing the chaotic nature of these influences (turbulent diffusion). The components of $\vec{L}(t)$ are independent random variables with zero expected mean.

Particle displacement under the effect of turbulent diffusion effect can be represented as a Markov process, in which predicting the subsequent position of the particle requires only information about its current state. Random fluctuations in this process are described by a Wiener process, which is a function of a normally distributed random variable with zero expected mean and dispersion – *dt*. The relation between equation (1) and the advection-diffusion equation is demonstrated through the Kolmogorov forward equation (or Fokker–Planck equation) in works [7] [1]. According to work [6], the Lagrangian particle transport equation along the three coordinate axes can then be expressed as follows:

$$\begin{aligned} dx^l(t) &= u(\vec{x}, t)dt + \frac{\partial K_x(\vec{x},t)}{\partial x}dt + \xi_x\sqrt{2K_x(\vec{x}, t)dt}, \\ dy^l(t) &= v(\vec{x}, t)dt + \frac{\partial K_y(\vec{x},t)}{\partial y}dt + \xi_y\sqrt{2K_y(\vec{x}, t)dt}, \\ dz^l(t) &= w(\vec{x}, t)dt + \frac{\partial K_z(\vec{x},t)}{\partial z}dt + \xi_z\sqrt{2K_z(\vec{x}, t)dt}, \end{aligned} \quad (2)$$

where u, v, w are velocity vector components; K_x, K_y, K_z are turbulent diffusion coefficients; ξ_x, ξ_y, ξ_z are independent, normally distributed random variables with a zero mean and unit dispersion. Note that the second term on the right-hand side of equations (2) has been introduced artificially to compensate for the unrealistic particle accumulation in regions of low diffusivity [6] [23, 24], ensuring that turbulent diffusion processes are modelled correctly within the framework of the advection-diffusion equation.

We introduced several modifications to the aforementioned Lagrangian particle transport model to optimize it for the processes of interest. Firstly, in the context of an eddy-resolving ocean model, the effects of horizontal turbulent diffusion can be disregarded, as advective processes largely dominate weak horizontal plane fluctuations [6]. Secondly, studies [8] [24] suggest that the vertical turbulent diffusion term, which is responsible for random fluctuations, should be adjusted to second-

[7] Wolk, F., 2003. *Three-Dimensional Lagrangian Tracer Modelling in Wadden Sea Areas: Diploma Thesis*. Hamburg, Germany: Carl von Ossietzky University Oldenburg, 77 p.

[8] Ermak, D.L., Nasstrom, J.S. and Taylor, A.G., 1995. *Implementation of a Random Displacement Method (RDM) in the ADPIC Model Framework.* Lawrence Livermore National Laboratory, 16 p. (Report UCRL-ID-121742). https://doi.org/10.2172/103520

order accuracy. This improves the representation of diffusive processes in the bottom boundary layer, where K_z approaches zero. Thirdly, in practice, the presence of dissolved substances in a given volume alters the density of the solution. In most cases, however, this can be disregarded. In certain applications, particularly those involving long-term simulations or significant concentrations of passive tracers (such as sediment transport studies [6]), the effect of buoyancy variation may become non-negligible. To account for this, an additional term has been introduced into the third equation (2) to describe particle motion along the vertical axis at a constant velocity w^s, reflecting this process in the first-order approximation. Considering all these modifications, the final system of Lagrangian particle transport equations takes the following form:

$$\begin{aligned} dx^l(t) &= u^o(\vec{x},t)dt, \\ dy^l(t) &= v^o(\vec{x},t)dt, \\ dz^l(t) &= (w^o(\vec{x},t) + w^s)dt + \frac{\partial K_z(\vec{x},t)}{\partial z}dt + \\ &+\xi_z\sqrt{2K_z(\vec{x},t)dt + \left(\frac{\partial K_z(\vec{x},t)}{\partial z}dt\right)^2}, \end{aligned} \tag{3}$$

where u^o, v^o, w^o are components of the fluid velocity vector at a given coordinate point.

According to [1], it is particularly noteworthy that there are currently no publicly available implementations of synchronous Lagrangian-Eulerian ocean models that can compute particle trajectories based on stochastic differential equations, explicitly accounting for turbulent diffusion. Furthermore, we have been unable to find ocean circulation models that support Lagrangian particle transport in this formulation. In this respect, the particle transport functionality in the INMIO model is unique.

Equations of the form (3) only apply to particle transport in a liquid ocean environment where turbulent diffusion is caused by mesoscale vortex processes. However, if a particle becomes trapped in an ice cover, turbulent mixing is absent. In this case, particles move along the ice velocity vector. This motion can be described by a simple Lagrangian transport equation:

$$\begin{aligned} dx(t) &= u^i(\vec{x},t)dt, \\ dy(t) &= v^i(\vec{x},t)dt, \\ dz(t) &= 0, \end{aligned} \tag{4}$$

where u^i, v^i are the horizontal components of the ice velocity. Since our model does not consider particle transport processes beyond the ocean surface, vertical particle movement in the ice cover can be disregarded. The transition between oceanic and ice-bound transport modes occurs when particles cross the ice-ocean interface, which requires special treatment in numerical implementations to ensure the conservation of particle properties. In this case, the moment at which particles transition into and out of a frozen state can be estimated using a probabilistic approach based on the intensity of ice formation and melting processes.

As noted earlier, the ocean – ice modeling system comprises two models that are managed by the compact computational platform CMF3.0. This enables each model to obtain the necessary information from the other with a specified discreteness. Within the framework of Lagrangian transport in a two-phase

environment, our focus is on the ice velocity field, as well as on the potential for ice formation and melting. The first quantity will obviously be used directly in equations (4) to calculate particle displacement. The second quantity, the ice formation and melting potential, determines the procedures in the ice model for forming frozen structures on the ocean surface. When this quantity is positive, it indicates that the water temperature has fallen below the freezing point. This leads to the formation of ice proportional to the magnitude of the potential, and the subsequent accumulation of ice crystals on the surface, gradually forming an ice cover. Negative potential values correspond to melting processes. In dimensionless form, this parameter enables the approximate estimation of the probability of a Lagrangian particle freezing or thawing if it is located in the ocean surface layer:

$$P(\vec{x}, t) = \left|1 - \frac{T^{o}(\vec{x},t)}{T^{f}(\vec{x},t)}\right|, \quad (5)$$

where T^{o} is the fluid temperature at the current coordinates of the Lagrangian particle; T^{f} is the freezing temperature at that point; formula (5) defines the probability function for particle freezing if it is located in the surface layer when $T^{o} < T^{f}$, as well as the probability function for particle thawing if it was already frozen when $T^{o} \geq T^{f}$.

Thus, the general model of Lagrangian transport in the quasi-two-phase ocean – ice environment can be represented as follows:

1. If the particle is in a frozen state, its movement is described by equations (4) and the probability of thawing is determined by function (5) when $T^{o} \geq T^{f}$.

2. Otherwise, the particle moves freely in the liquid phase according to equations (3) and may freeze with a probability (5) if located in the surface layer of the fluid (in the uppermost grid cell of the numerical model) when $T^{o} < T^{f}$.

This approach enables the model to be implemented without the need to transfer particle information to the ice model. This significantly reduces the number of computational resources required and simplifies the program code simultaneously.

For the numerical integration of the equations describing the transport of Lagrangian particles, the explicit Euler scheme or Runge–Kutta schemes [1] of various orders of accuracy are typically used. In the autonomous implementation of coupled models, when temporal discretization of the velocity field is relatively coarse, higher-order time approximation schemes are employed to enhance the accuracy of particle trajectory reconstruction in the original equations (3) and (4). In such cases, methods such as Heun scheme and fourth-order (or higher) Runge–Kutta schemes [6] are commonly applied [1, 25].

In coupled models, the requirement for high-order temporal schemes becomes less critical, enabling the use of the first-order accurate Euler scheme. The accuracy of the numerical integration of the original equations can be adjusted by reducing the time step in the numerical implementation of the Lagrangian model. Numerical tests of particle transport in a static circular current field demonstrate that, regardless of the numerical scheme used (Euler or Runge–Kutta), the integration time step in the Lagrangian transport model must be significantly smaller than in the ocean model to achieve acceptable accuracy in reconstructing circular particle trajectories [1]. Thus, the finite-difference scheme for the original Lagrangian particle transport

equations in the velocity field of the coupled ocean – ice modeling system can be expressed as follows:

$$
\begin{gathered}
x_{n+1}^l = x_n^l + \begin{cases} u^o(\overrightarrow{x_n})\Delta t^l, & s = \text{ocean}, \\ u^i(\overrightarrow{x_n})\Delta t^l, & s = \text{ice}, \end{cases} \\
y_{n+1}^l = y_n^l + \begin{cases} v^o(\overrightarrow{x_n})\Delta t^l, & s = \text{ ocean}, \\ v^i(\overrightarrow{x_n})\Delta t^l, & s = \text{ice}, \end{cases} \\
z_{n+1}^l = z_n^l + \begin{cases} (w^o(\overrightarrow{x_n}) + w_s)\Delta t^l + \frac{\Delta K_z(\overrightarrow{x_n})}{\Delta z(\overrightarrow{x_n})}\Delta t^l + \\ 0, \end{cases} \\
+ \begin{cases} \xi_z \sqrt{2K_z(\overrightarrow{x_n})\Delta t^l + \left(\frac{\Delta K_z(\overrightarrow{x_n})}{\Delta z(\overrightarrow{x_n})}\Delta t^l\right)^2}, & s = \text{ocean}, \\ 0 & s = \text{ice}, \end{cases} \\
P_n(s = \text{ice}) = 1 - \frac{T^o(\overrightarrow{x_n})}{T^f(\overrightarrow{x_n})}, s = \text{ocean}, T^o \le T^f, z_n^l < z_2, \\
P_n(s = \text{ocean}) = \frac{T^o(\overrightarrow{x_n})}{T^f(\overrightarrow{x_n})} - 1, s = \text{ice}, T^o > T^f, \\
\Delta t^l = \Delta t^o / p,
\end{gathered}
\tag{6}
$$

where $\overrightarrow{x_n} = \{x_n^l, y_n^l, z_n^l\}$ is the Lagrangian particle coordinate at the *n*-th integration step; $\overrightarrow{u^o} = \{u^o(\overrightarrow{x_n}), v^o(\overrightarrow{x_n}), w^o(\overrightarrow{x_n})\}$ is current velocity at the point with particle coordinates; $\overrightarrow{u^i} = \{u^i(\overrightarrow{x_n}), v^i(\overrightarrow{x_n}), 0\}$ is ice movement velocity; Δt^l is the time step in the Lagrangian model; Δt^o is the time step in the ocean model; p is the integer determining the refinement factor for the Lagrangian model integration order relative to the INMIO model. Test calculations demonstrate that acceptable solution accuracy is achieved at $p \sim 10$.

Interpolation in the Lagrangian particle transport model. The Lagrangian transport modeling involves the movement of particles in a space of continuously defined coordinates (6). This means that, at any given moment, the coordinates of particles may not coincide with those of the grid nodes in the computational domain of the numerical model. Therefore, to achieve greater accuracy, the discrete velocity field of the ocean – ice system must be reconstructed within computational cells. This is typically accomplished using interpolation methods of various orders [1]. In this study, linear interpolation was chosen as it is the most computationally efficient approach while still providing acceptable accuracy [25].

However, applying this approach is complicated by the fact that the INMIO model equations are formulated in an arbitrary orthogonal coordinate system in the horizontal plane. In such a configuration, determining particle positions on the computational grid and performing interpolation becomes non-trivial. One solution to this problem, which preserves the simplicity of linear interpolation formulas, is to consider particle transport equations in logical (computational) space (Fig. 2) [25].

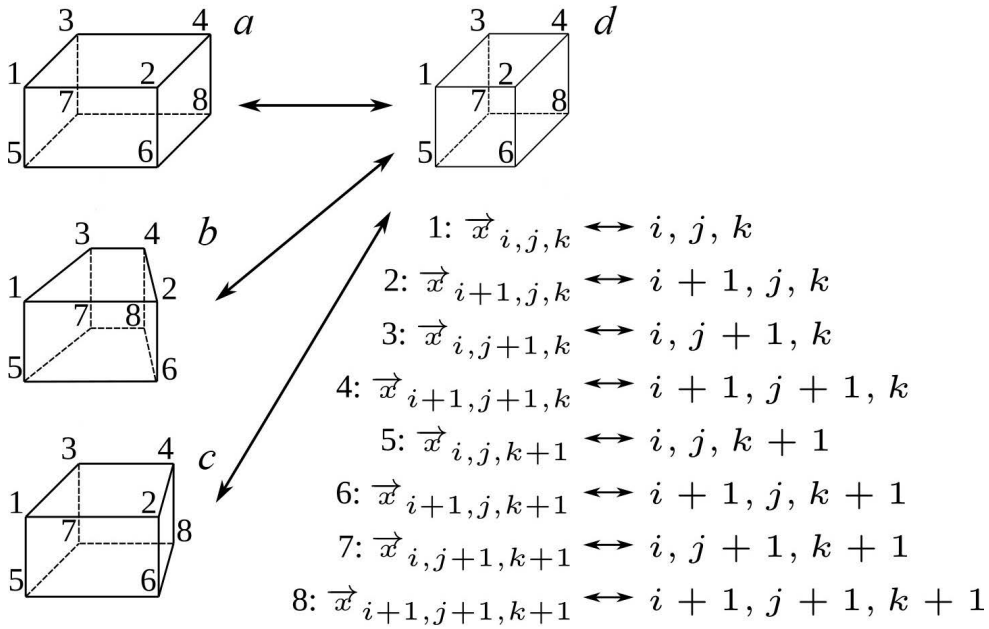

F i g. 2. Display of computational cells in different coordinate systems: Cartesian (*a*), polar (*b*), bipolar (*c*) and semi-logical (*d*) ones

This space is a Cartesian coordinate system that arises naturally during the implementation of most numerical models. It is described by the indices of grid nodes. However, the transition to logical coordinates is only meaningful in the horizontal plane, since the INMIO model introduces *z*-coordinates in the vertical plane. In this new semi-logical space, $\bar{C}$ point coordinates can be represented as $\vec{\xi} = \{\xi, \eta, z\}$, where $\xi = i + \alpha$ and $\eta = j + \beta$, and the mapping function from this space to physical space *P* takes the following form:

$$\begin{gathered}\tau\left(f_{i,j,k}, \xi, \eta, z\right) = \sum_{I,J,K=0}^{1} f_{i+I,j+J,k+K}\varphi_I(\alpha)\psi_J(\beta)\chi_{k+K}(z), \\ \varphi_0(\alpha) = (1-\alpha), \varphi_1(\alpha) = \alpha, \alpha \in [0,1], \\ \psi_0(\beta) = (1-\beta), \psi_1(\beta) = \beta, \beta \in [0,1], \\ \chi_k(z) = \frac{z_{k+1}-z}{z_{k+1}-z_k}, \chi_{k+1}(z) = \frac{z-z_k}{z_{k+1}-z_k}, z \in [z_k, z_{k+1}],\end{gathered} \tag{7}$$

where *i*, *j*, *k* are indices of the computational grid cell; α, β are the real-valued displacements of a point in logical space relative to the cell index; $f_{i,j,k}$ is the function that defines the parameter values at the grid nodes in physical space; φ, ψ, χ are the basic mapping functions. When the function *f* specifies the coordinates of the grid cell nodes in physical space, expression (7) can be used to compute physical coordinates from given semi-logical coordinates. If *f* represents velocity vectors, expression (7) performs trilinear velocity interpolation within the specified grid cell (see Fig. 1).

However, when transitioning to semi-logical space, the particle motion vector should be rescaled according to the spatial deformation of the corresponding coordinate axes. Following [25], this rescaling can be implemented through the following transformation within the previously defined mapping framework:

$$\vec{u} = J \cdot \vec{\omega}, \vec{\omega} = J^{-1} \cdot \vec{u},$$
$$J = \left(\frac{\partial \vec{x}}{\partial \xi} \middle| \frac{\partial \vec{x}}{\partial \eta} \middle| \frac{\partial \vec{x}}{\partial z}\right), \quad (8)$$

where $\vec{u} = \{u, v, w\}$ is the velocity vector in physical space; $\vec{\omega} = \{\tilde{u}, \tilde{v}, w\}$ is the velocity vector in semi-logical space; J is the Jacobian matrix that defines the spatial deformation during transformation from physical to semi-logical coordinates.

On a discrete grid, the Jacobian matrix J can be computed using finite differences. However, as demonstrated in [25], maximum accuracy requires these differences to be calculated for all nodes of the computational cell using both forward and backward finite difference schemes. This can be achieved using the mapping function $\tau(\vec{x}, \xi, \eta, z)$ (7), which defines the transformation from semi-logical to physical coordinates. It is straightforward to show that, in the third column and in the third row of the Jacobian matrix, all elements except the last one will be zero, since the given mapping does not affect the *OZ* axis. For each computational cell (*i*, *j*, *k*) the matrix will therefore take the form:

$$J_{i,j,k} = \begin{pmatrix} \frac{\partial \tau(x)}{\partial \alpha} & \frac{\partial \tau(x)}{\partial \beta} & 0 \\ \frac{\partial \tau(y)}{\partial \alpha} & \frac{\partial \tau(y)}{\partial \beta} & 0 \\ 0 & 0 & 1 \end{pmatrix}, \quad (9)$$

where partial derivatives are calculated trivially for the mapping function $\tau(\vec{x}, \xi, \eta, z)$ of form (7).

Equations (6) remain invariant under the above mapping since the *OZ* dimension remains unchanged. To obtain the Lagrangian particle coordinates at the next time point, it is sufficient to scale the velocity vector at the cell nodes using formulas (8) and (9), interpolate it to the particle coordinates using formula (7), and then apply the semi-logical coordinates and resulting velocity vector directly to equations (6).

Results and discussion

Test calculations of particle transport in a static vortex field. As various aspects of the mathematical model presented above have been repeatedly verified in previous studies [6, 7] [1, 24], the primary objective of these test calculations is to demonstrate the correct implementation of the Lagrangian transport model and its integration methods on grids supported by the INMIO ocean model, in both Cartesian and geospheric/tripolar coordinate systems.

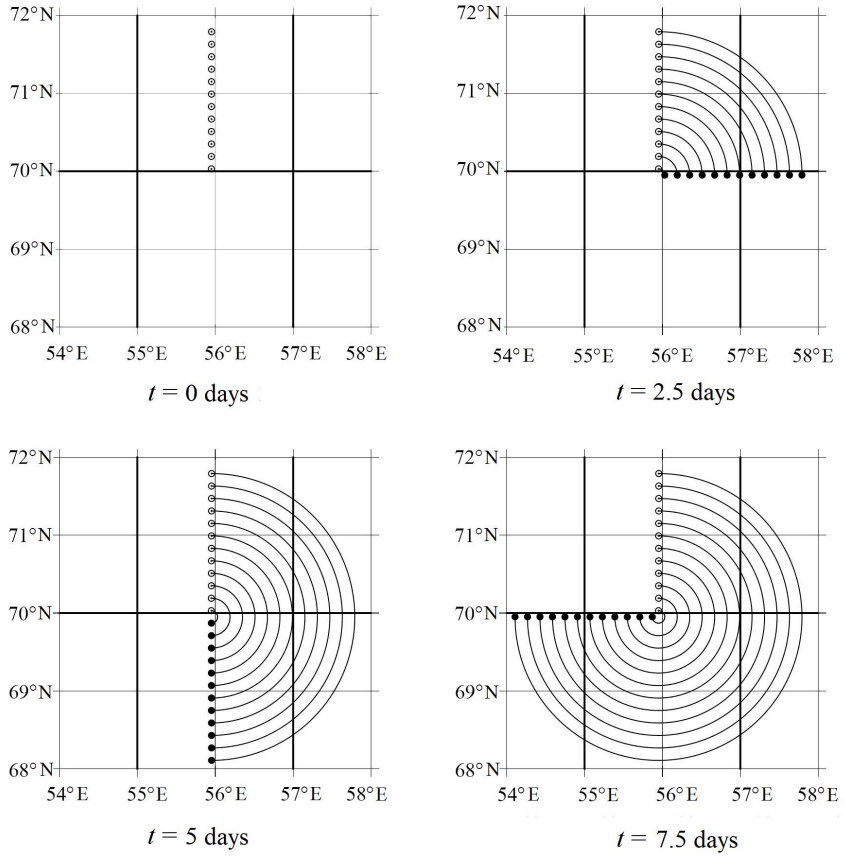

F i g. 3. Trajectories of particles moving in the static vortex field on a grid in the Cartesian coordinate system

The INMIO software model was configured to simulate a geographical domain within the rectangle defined by the coordinates 53°–59°E and 68°–72°N. To test particle transport, an artificial velocity field representing a static vortex centered in the middle of the domain was introduced. The vortex had a rotation period of ~ 10 days (angular velocity $W = 7.27 \cdot 10^{-6}$ rad/s). In the implementation of the Cartesian coordinate system, the linear velocity field was expressed in geographical units (degrees/seconds). In the spherical coordinate system, the velocity field dimensions corresponded to the metric system (m/s) and represented a vortex with the specified angular velocity centered on the Earth's surface at the aforementioned geographical coordinates. The model was discretized using a 60 × 40 computational grid with a resolution of 0.1°. The ocean model time step was set to $\Delta t^o = 6'$. The temporal discretization of the Lagrangian model was varied to obtain the most accurate particle trajectories. As expected, the particle trajectories formed concentric streamlines for this preset velocity field.

The computation was performed in parallel mode using six cores. Fig. 3 presents the results of the Lagrangian particle transport test calculation on the Cartesian grid.

As expected, the particles move synchronously in a circle along the streamlines specified in the computational domain of the vortex velocity field. It is obvious that particle transitions between grid cells and computational domains (indicated by thick lines in Fig. 3) do not distort their trajectories, and their motion in a vortex with a ~10-day period is reflected in the particle coordinates. The trajectories shown in Fig. 3 were obtained using $p = 5$ in expressions (6).

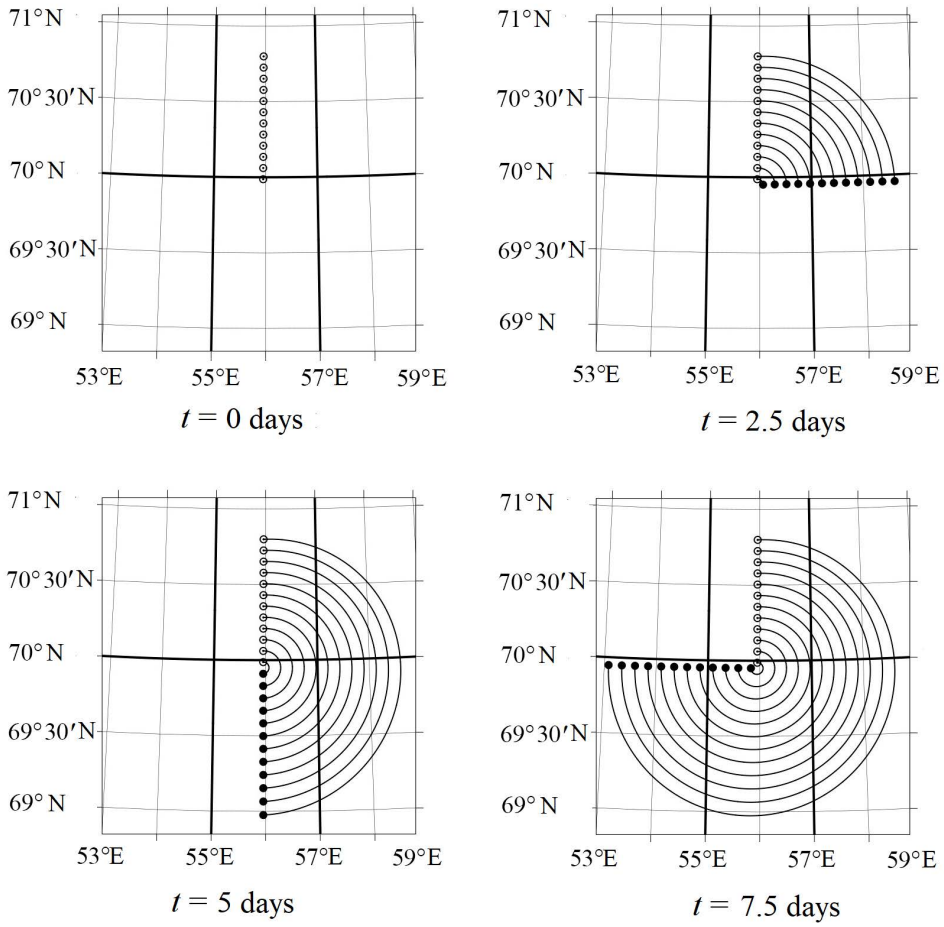

F i g. 4. Trajectories of particles moving in the static vortex field on a grid in the geographic coordinate system

In the next numerical test, the particles moved on a grid in a geographic coordinate system.

Fig. 4 shows the results of calculations at various stages of the modeling process. As in the previous case, the particles move synchronously along the streamlines of the vortex velocity field. The trajectories remain circular in metric

space representation only. They no longer appear as circles in geographical coordinates, but instead manifest as elongated ellipsoidal curves elongated along the latitudinal axis. As before, the trajectories shown in Fig. 4 were obtained using $p = 5$ in equations (6).

To obtain more accurate Lagrangian particle trajectories, special consideration must be given to particle transitions between computational cells, including transfers between subdomains in the two-dimensional decomposition of the ocean model's computational domain. In the former instance, this is due to the peculiarities of modeling in semi-logarithmic space, where the velocity field at cell boundaries is no longer continuous (equations (7) and (8)). Therefore, to achieve maximum accuracy, the particle velocity and path should be recalculated when crossing cell boundaries. This requirement also applies when modeling in physical space, albeit for different reasons. In our implementation, this condition is only partially satisfied by using a time integration step (6) that is smaller than the ocean model time step. Conversely, 'seamless' particle transfer between computational domains would indicate the correct implementation of the parallel computation algorithm for the Lagrangian model.

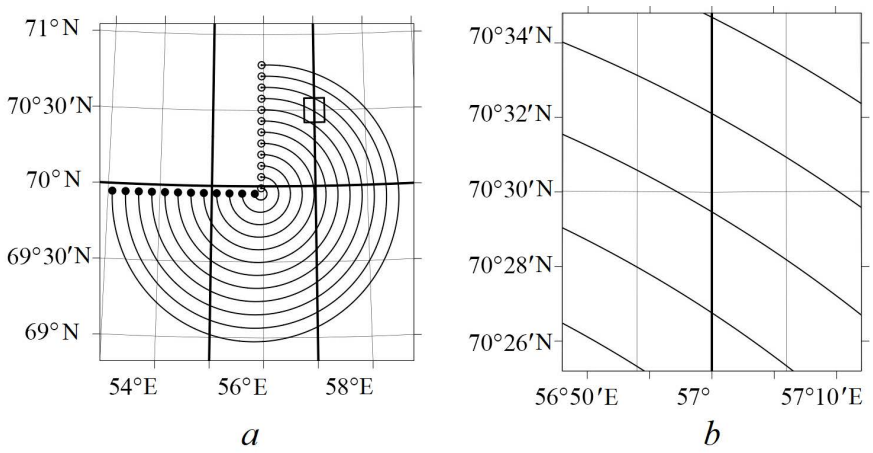

F i g. 5. Particle trajectories in the test experiment on a grid in the geographic coordinate system (rectangle highlights the region on the boundary of computational cells and calculation domain) (*a*), enlarged image of the highlighted area (*b*)

Fig. 5 shows, for example, particle trajectories crossing boundaries between two computational subdomains and several grid cells. As can be seen, the trajectories demonstrate no visible discontinuities. This indicates firstly that the required level of accuracy has been achieved for the specified Δt^l ($p = 5$ in equations (6)) and secondly that the interprocessor particle exchange in the parallel Lagrangian transport model has been implemented correctly.

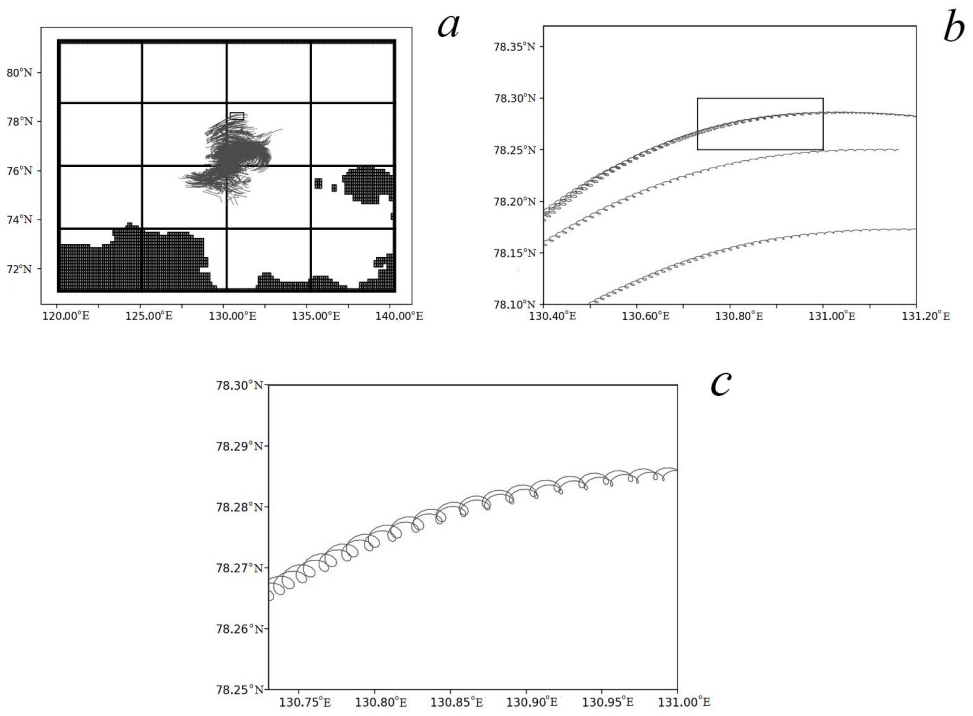

F i g. 6. Particle trajectories in the Laptev Sea current model (the study area is shown by a rectangle) (*a*), enlarged image of the indicated area (rectangle highlights the zone of interest) (*b*), enlarged image of the highlighted area (*c*)

Test calculation of particle transport in the coupled ocean – ice model. The main purpose of this test calculation was to demonstrate the correct implementation of the above-described Lagrangian model within the ocean – ice modeling system consisting of the INMIO ocean model and the CICE5.1 ice thermodynamics model. The configuration of the ocean model for the AO was adopted from [6], but the Laptev Sea (71°–91°N, 120°–140°E) was chosen as the model domain because its waters are ice-covered for most of the year. The model bathymetry was interpolated from ETOPO5 [9] data. Atmospheric forcing was specified according to the conditions of the international CORE-I experiment [26] as a normal annual cycle. The horizontal computational grid for the ocean and ice models was defined using a spherical coordinate system with 160×80 nodes horizontally and 49 vertical levels. Thus, the coupled ocean – ice model operated at a resolution of 0.125°. The integration step was set identically for the ocean and ice models at $\Delta t^o = \Delta t^i = 5'$. In the Lagrangian model, the integration step was set to $\Delta t^l = 1'$, and particle coordinates were saved at the same frequency. Physical field

[9] National Oceanic and Atmospheric Administration (NOAA), 1988. *Digital Relief of the Surface of the Earth*. Data Announcement 88-MGG-02. National Geophysical Data Center, Boulder, Colorado.

data, including ice velocity fields, were synchronized every 10′ in the coupled ocean – ice system. The ocean – ice system took 1 year to setup; after this, the Lagrangian model was activated synchronously for an additional two model months for 10^4 particles initially located in the surface layer at 76°N, 130°E. The calculation was performed in parallel mode using 16 computational cores for the ocean model.

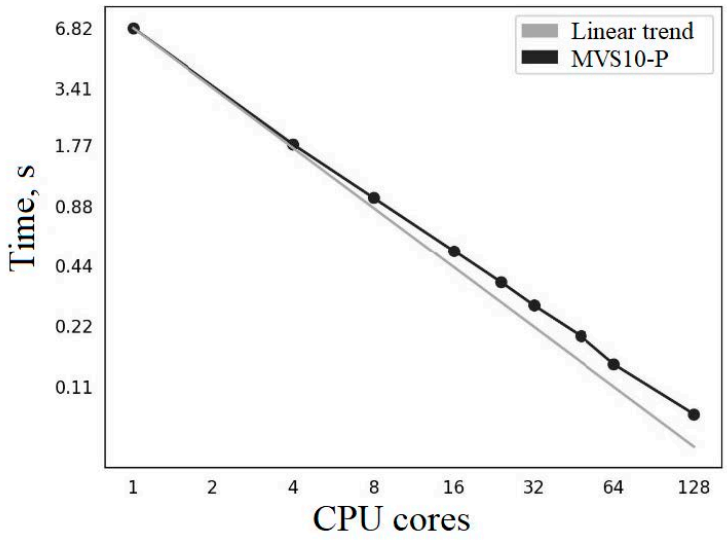

F i g. 7. Graph of the dependence of one step duration (in seconds) in the Lagrangian model upon the core number in the experiment with uniform particle distribution in the simulated region

Fig. 6, a displays horizontal trajectories of particles after two months of coupled numerical integration of the ocean – ice dynamics model and the Lagrangian transport model. As can be seen, the particles follow different trajectories under the effect of internal currents, as expected for a model incorporating turbulent mixing effects. Fig. 6, *b* presents an enlarged view of the trajectories of several particles within the rectangular area indicated in Fig. 6, *a*. The shapes of the trajectories reflect two primary dynamic processes: a quasi-uniform process in the selected region and circular motions corresponding to inertial oscillations in the current field. A further magnification (Fig. 6, *c*) reveals the synchronous horizontal movement of two nearby particles.

To evaluate the scalability of the implementation of the Lagrangian transport model, we performed a series of numerical experiments involving 10^6 particles that were uniformly distributed over the surface of the domain that was simulated in these experiments (Fig. 7). As can be seen, the dependence of the time taken to calculate

one step in the Lagrangian transport model on the number of computing cores is almost linear, indicating good scalability of the parallel algorithm implemented for calculating the Lagrangian transport. However, it should be noted that this only holds true for the case of uniformly distributed particles, which rarely occurs in actual simulations. Under the influence of currents, particle concentrations within computational domains are not constant, but evolve over time. Consequently, the total computation time per integration step in the Lagrangian model is determined by the domain containing the maximum number of particles.

Conclusion

This study presents a Lagrangian particle transport model for the quasi-two-phase ocean – ice medium that incorporates vertical turbulent mixing. This model has been implemented in the INMIO ocean general circulation model, which uses arbitrary horizontal coordinate systems. The model's ability to support both two-phase dynamics and turbulent diffusion is a unique feature among existing ocean dynamics models. This modeling tool is particularly relevant given the ongoing intensive development of the Arctic region.

The model implementation supports the parallel computation of the transport of a large number of particles (up to 10^6) within the framework of a two-dimensional decomposition of the computational domain. For uniformly distributed Lagrangian particles, the algorithm demonstrates near-linear scalability. The particle trajectory calculations are performed on the computational cores of the ocean model, which determines the maximum number of particles. Otherwise, having more than 10^6 particles concentrated in one computational domain will inevitably lead to an imbalance in the computational load, negatively affecting the model's performance. However, this worst-case scenario is unlikely, occurring only at the initial moment when particles are concentrated in specific domains according to the conditions of the problem. As the numerical solution evolves, the particles will inevitably be transported to different parts of the computational domain, a process that will be further accelerated by turbulent mixing.

The developed interprocessor exchange algorithm ensures the correct transfer of particle data between subdomains of computing cores, and guarantees the possibility of particle transport throughout the entire ocean model domain. Test calculations demonstrate that setting the integration time step to one-fifth of the ocean model's time step achieves relative trajectory smoothness when crossing the cell boundaries.

REFERENCES

1. Van Sebille, E., Griffies, S.M., Abernathey, R., Adams, T.P., Berloff, P., Biastoch, A., Blanke, B., Chassignet, E.P., Cheng, Y. [et al.], 2018. Lagrangian Ocean Analysis: Fundamentals and Practices. *Ocean Modelling*, 121, pp. 49-75. https://doi.org/10.1016/j.ocemod.2017.11.008

2. Khvostova, M.S., 2018. Environmental Problems of Operation of Floating Nuclear Power Plant in the Arctic Region. *Russian Arctic*, (1), pp. 11-29 (in Russian).

3. Antipov, S.V., Bilashenko, V.P., Vysotskii, V.L., Kalantarov, V.E., Kobrinskii, M.N., Sarkisov, A.A., Sotnikov, V.A., Shvedov, P.A., Ibraev, R.A. [et al.], 2015. Prediction and Evaluation of the Radioecological Consequences of a Hypothetical Accident on the Sunken Nuclear Submarine B-159 in the Barents Sea. *Atomic Energy*, 119(2), pp. 132-141. https://doi.org/10.1007/s10512-015-0039-x

4. Ushakov, K.V., Ibrayev, R.A. and Kalmykov, V.V., 2015. Simulation of the World Ocean Climate with a Massively Parallel Numerical Model. *Izvestiya, Atmospheric and Oceanic Physics*, 51(4), pp. 362-380. https://doi.org/10.1134/S0001433815040131

5. Kalmykov, V.V., Ibrayev, R.A., Kaurkin, M.N. and Ushakov, K.V., 2018. Compact Modeling Framework v3.0 for High-Resolution Global Ocean–Ice–Atmosphere Models. *Geoscientific Model Development*, 11(10), pp. 3983-3997. https://doi.org/10.5194/gmd-11-3983-2018

6. Kalnitskii, L.Y., Kaurkin, M.N., Ushakov, K.V. and Ibrayev, R.A., 2020. Seasonal Variability of Water and Sea Ice Circulation in the High-Resolution Model of the Arctic Ocean. Известия Российской академии наук. *Izvestiya. Atmospheric and Oceanic Physics*, 56(5), pp. 598-610. https://doi.org/10.31857/S0002351520050065 (in Russian).

7. Kulakov, M.Yu., Makshtas, A.P. and Shutilin, S.V., 2012. AARI–IOCM – Coupled Ice-Ocean Circulation Model for the Arctic Ocean. *Arctic and Antarctic Research*, 2(92), pp. 6-18 (in Russian).

8. Campin, J.-M., Marshall, J. and Ferreira, D., 2008. Sea Ice-Ocean Coupling Using a Rescaled Vertical Coordinate z*. *Ocean Modelling*, 24(1-2), pp. 1-14. https://doi.org/10.1016/j.ocemod.2008.05.005

9. Fadeev, R.Yu., Ushakov, K.V., Tolstykh, M.A. and Ibrayev, R.A., 2018. Design and Development of the SLAV-INMIO-CICE Coupled Model for Seasonal Prediction and Climate Research. *Russian Journal of Numerical Analysis and Mathematical Modelling*, 33(6), pp. 333-340. https://doi.org/10.1515/rnam-2018-0028

10. Warner, J.C., Armstrong, B., He, R. and Zambon, J.B., 2010. Development of a Coupled Ocean–Atmosphere–Wave–Sediment Transport (COAWST) Modeling System. *Ocean Modelling*, 35(3), pp. 230-244. https://doi.org/10.1016/j.ocemod.2010.07.010

11. Döös, K., Jönsson, B. and Kjellsson J., 2017. Evaluation of Oceanic and Atmospheric Trajectory Schemes in the TRACMASS Trajectory Model v6.0. *Geoscientific Model Development*, 10(4), pp. 1733-1749. https://doi.org/10.5194/gmd-10-1733-2017

12. Blanke, B. and Raynaud, S., 1997. Kinematics of the Pacific Equatorial Undercurrent: An Eulerian and Lagrangian Approach from GCM Results. *Journal of Physical Oceanography*, 27(6), pp. 1038-1053. https://doi.org/10.1175/1520-0485(1997)027<1038:KOTPEU>2.0.CO;2

13. Paris, C.B., Helgers, J., Van Sebille, E. and Srinivasan, A., 2013. Connectivity Modeling System: A Probabilistic Modeling Tool for the Multiscale Tracking of Biotic and Abiotic Variability in the Ocean. *Environmental Modelling & Software*, 42, pp. 47-54. https://doi.org/10.1016/j.envsoft.2012.12.006

14. Golubeva, E. and Gradova, M., 2024. Numerical Study of the Riverine Microplastic Distribution in the Arctic Ocean. *Water*, 16(3), 441. https://doi.org/10.3390/w16030441

15. Bleck, R., 2002. An Oceanic General Circulation Model Framed in Hybrid Isopycnic-Cartesian Coordinates. *Ocean Modelling*, 4(1), pp. 55-88. https://doi.org/10.1016/S1463-5003(01)00012-9

16. Shchepetkin, A.F. and McWilliams, J.C., 2005. The Regional Oceanic Modeling System (ROMS): A Split-Explicit, Free-Surface, Topography-Following-Coordinate Oceanic Model. *Ocean Modelling*, 9(4), pp. 347-404. https://doi.org/10.1016/j.ocemod.2004.08.002

17. Marshall, J., Adcroft, A., Hill, C., Perelman, L. and Heisey, C., 1997. A Finite-Volume, Incompressible Navier Stokes Model for Studies of the Ocean on Parallel Computers. *Journal of Geophysical Research: Oceans*, 102(C3), pp. 5753-5766. https://doi.org/10.1029/96JC02775

18. Ibrayev, R.A., Khabeev, R.N. and Ushakov, K.V., 2021. Eddy-Resolving 1/10° Model of the World Ocean. *Izvestiya, Atmospheric and Oceanic Physics*, 48(1), pp. 37-46. https://doi.org/10.1134/S0001433812010045

19. Kalmykov, V.V. and Ibrayev, R.A., 2013. A Framework for the Ocean-Ice-Atmosphere-Land Coupled Modeling on Massively-Parallel Architectures. *Numerical Methods and Programming*, 14(3), pp. 88-95 (in Russian).

20. Maier-Reimer, E. and Sündermann, J., 1982. On Tracer Methods in Computational Hydrodynamics. In: M.B. Abbot and J.A. Cunge, eds., 1982. *Engineering Applications of Computational Hydroulics*. Boston, London, Melbourne: Pitman Advanced Publishing Program. Vol. 1, pp. 198-217.

21. Gardiner, C.W., 1985. *Handbook of Stochastic Methods for Physics, Chemistry and the Natural Sciences*. Springer Series in Synergetics, vol. 13. Berlin, Heidelberg: Springer Berlin Heidelberg, 439 p. https://doi.org/10.1007/978-3-662-02452-2

22. Hunter, J.R., Craig, P.D. and Philips, H.E., 1993. On the Use of Random Walk Models with Spatially Variable Diffusivity. *Journal of Computational Physics*, 106(2), pp. 366-376. https://doi.org/10.1016/S0021-9991(83)71114-9

23. Visser, A.W., 1997. Using Random Walk Models to Simulate the Vertical Distribution of Particles in a Turbulent Water Column. *Marine Ecology Progress Series*, 158, pp. 275-281. https://doi.org/10.3354/meps158275

24. Sunarko and Zaki Su'ud, 2016. Lagrangian Particle Method for Local Scale Dispersion Modeling. *Journal of Physics: Conference Series*, 739, 012122. https://doi.org/10.1088/1742-6596/739/1/012122

25. Sadarjoen, A., Van Walsum, T., Hin, A.J.S. and Post, F.H., 1994. Particle Tracing Algorithms for 3D Curvilinear Grids. In: G. Nielson, H. Müller and H. Hagen, eds., 1994. *Scientific Vizualization. Overviews. Methodologies. Techniques*. Delft University of Technology, pp. 299-323.

26. Griffies, S.M., Biastoch, A., Böning, C., Bryan, F., Danabasoglu, G., Chassignet, E.P., England, M.H., Gerdes, R., Haak, H. [et al.], 2009. Coordinated Ocean-Ice Reference Experiments (COREs). *Ocean Modelling*, 26(1-2), pp. 1-46. https://doi.org/10.1016/j.ocemod.2008.08.007

Submitted 25.11.2024; approved after review 04.01.2024;
accepted for publication 13.03.2025.

About the authors:

Sergey V. Semin, Research Associate, Shirshov Institute of Oceanology, Russian Academy of Sciences (36 Nakhimovskiy ave., Moscow, 117997, Russian Federation) Engineer, Nuclear Safety Institute, Russian Academy of Sciences (52 Bolshaya Tulskaya Str., Moscow, 115191, Russian Federation), CSc. (Phys.-Math.), **Scopus Author ID: 56604365800**, **ORCID ID: 0000-0001-8079-168X**, **ResearcherID: ABH-7440-2020**, svsemin@unistemlab.com

Leonid Yu. Kalnitskii, Leading Engineer, Shirshov Institute of Oceanology, Russian Academy of Sciences (36 Nakhimovskiy ave., Moscow, 117997, Russian Federation), **Scopus Author ID: 57219609143, ORCID ID: 0009-0005-4023-2257**, leonid.kalnitsckij@yandex.ru

Konstantin V. Ushakov, Senior Research Associate, Shirshov Institute of Oceanology, Russian Academy of Sciences (36 Nakhimovskiy ave., Moscow, 117997, Russian Federation), CSc. (Phys.-Math.), **Scopus Author ID: 55015342700**, **ORCID ID: 0000-0002-8454-9927**, **ResearcherID: U-6185-2017**, ushakovkv@mail.ru

Rashit A. Ibrayev, Chief Research Associate, Marchuk Institute of Numerical Mathematics, Russian Academy of Sciences (8 Gubkina Str., Moscow, 119333, Russian Federation), Shirshov

Institute of Oceanology, Russian Academy of Sciences (36 Nakhimovskiy ave., Moscow, 117997, Russian Federation), DSc. (Phys.-Math.), Corresponding Member of RAS, **Scopus Author ID: 6602387822**, **ResearcherID: S-6750-2016**, **ORCID ID: 0000-0002-9099-4541**, ibrayev@mail.ru

Contribution of the co-authors:

Sergey V. Semin – development and adaptation of a Lagrangian model for arbitrary computational grids; integration of the model with the parallel Eulerian INMIO model for quasi-two-phase ocean dynamics; full model debugging; test calculations; processing and interpretation of data; preparation of text and graphical materials; text writing and paper maintenance

Leonid Yu. Kalnitskii – development of a Lagrangian particle model in a static vortex; test simulations in the static vortex and the Laptev Sea; data collection and processing; preparation of graphical materials

Konstantin V. Ushakov – development of the joint ocean-ice Laptev Sea model; participation in the discussions of the Lagrangian model development and the research results; interpretation of the joint sea-ice model calculation results; detailed paper review

Rashit A. Ibrayev – general scientific supervision of the research; formulation of goals and objectives of the study; advisory assistance in the model debug and development; results analysis and interpretation; article review and correction

The authors have read and approved the final manuscript.
The authors declare that they have no conflict of interest.